Journal of Applied Polymer Science

Synthesis of a PPV-fluorene derivative: Applications in luminescent devices

Paula C. Rodrigues,[1,2*] Bruno D. Fontes,[2] Bruno B. M. Torres,[1] Washington S. Sousa,[1] Gregório C. Faria,[1] Debora T. Balogh,[1] Roberto M. Faria,[1] Leni Akcelrud[2]

[1]Grupo de Polímeros, IFSC, Universidade de São Paulo, São Carlos SP, Brazil

[2]LaPPS, Universidade Federal do Paraná, Curitiba PR, Brazil

*Present address: Departamento Acadêmico de Química e Biologia, DAQBi, Universidade Tecnológica Federal do Paraná, Curitiba, PR, Brazil

Correspondence to: P. C. Rodrigues (E-mail: paulac@utfpr.edu.br) and R. M. Faria (E-mail: faria@ifsc.usp.br); L. Akcelrud (E-mail: leni@leniak.net)

ABSTRACT: Synthesis of a polyfluorene/poly(p-phenylene vinylene) derivative, the Poly [(9,9′-di-hexylfluorenediylvinylene-alt-1,4-phenylenevinylene)-co-((9,9′-(3-t-butylpropanoate) fluorene-1,4-phenylene)] (LaPPS 42) was performed following Wittig and Suzuki routes. Polyfluorenes and derivatives have been used in electroluminescent devices, and the synthesis described here has the advantage in pave the way to get distinct structures having different emission spectra. An extensive study of its electrochemical, thermomechanical, optical, and structural properties was carried out, as well as its application in electroluminescent devices. Polymer light-emitting diodes (PLEDs) and polymer light-emitting electrochemical cells (PLECs) were built using LaPPS 42 as active layer, and their electric and optical characterizations confirm they have a potential as active element in electroluminescent devices. © 2015 Wiley Periodicals, Inc. J. Appl. Polym. Sci. **2015**, *132*, 42579.

KEYWORDS: conducting polymers; photochemistry; properties and characterization

Received 18 November 2014; accepted 4 June 2015

DOI: 10.1002/app.42579

INTRODUCTION

High-efficiency organic light-emitting devices and low-cost production of flexible displays have encouraged the search for new luminescent polymer structures. A desirable polymer light-emitting device should have low operating voltage, high exciton generation efficiency and high power efficiency.

Derivatives and copolymers of polyfluorene have been extensively used for electroluminescent devices mainly because it is possible to tune the emission of the active layer through a variety of chemical modifications that can be introduced in the main chain.[1–5] Thus, modified polyfluorenes can cover a range of emission throughout the visible spectrum, exhibiting high electroluminescence efficiency, as well as good thermal and oxidative stabilities.

Polymer light-emitting diodes (PLEDs)[6–8] and polymer light-emitting electrochemical cells (PLECs)[9–12] are two types of organic devices for applications in lighting panels and screen displays. While PLEDs operate as single diodes whose performance depend on the bias polarity and on the work function of the electrodes, PLECs can light in both voltage polarities and do not depend on the characteristics of the electrodes.[10] These differences comes from the fact that in a LED the active region is a single layer of a luminescent polymer; in PLECs, on the other hand, the active layer is made by blending an electronic luminescent polymer with an ionic conducting polymer and a triflate salt.[10–12] Another difference resides in the mechanism of recombination and light emission. In PLEDs exciton recombination can occur throughout the length of the active layer; in PLECS, recombination occurs in a thin insulator region (*pin* junction) within the active layer, formed by *p* and *n* electrochemical doping.[10] One disadvantage of PLECs in comparison with PLEDs is the slow response caused by the low ionic mobility.

The present article brings a contribution to the synthesis of the poly[(9,9′-di-hexylfluorenediylvinylene-alt-1,4-phenylenevinylene)-co-((9,9′-(3-t-butylpropanoate) fluorene-1,4-phenylene)] (LaPPS 42), which is a copolymer based on fluorene and phenylenevinylene, and its application as the active layer in PLEDs and PLECs. The chemical route for the material's preparation followed the Wittig and Suzuki polycondensations, and an extensive study of its electrochemical, thermal and

thermomechanical, absorption–emission, and structural properties were presented. Finally, current–voltage and luminance–voltage characteristic curves of a PLED and a PLEC were obtained, showing the potential applications of LaPPS 42 in electroluminescent devices.

EXPERIMENTAL

Materials

The chemicals and solvents used were all purchased from Aldrich and used as received, without further purification, except when described in the specific chemical procedure.

Chemical Procedures

Synthesis of 2,7-bis[2-(4-bromophenyl)vinyl]-9,9-dihexyl-9H-fluorene (II). The compound was synthesized as described elsewhere.[13,14] In a round bottom necked flask it was added 500 mg (0.48 mmol) of 2,7-bis[(p-triphenylphosphonium)-methyl]-9,9-di-n-hexylfluorene dibromide (I), 195 mg (1.05 mol) of p-bromobenzaldehyde, and 23 mL of chloroform, under argon atmosphere. A solution of t-BuOK in anhydrous ethanol (268 mg, 2.4 mmol) was then added to the former mixture and the reaction allowed to proceed for 24 hours at 25°C. After that, 5 mL HCl 5% were added and the compound was precipitated by pouring the mixture into an excess of methanol. The material was purified with column chromatography using $CHCl_3$, giving a yellow viscous compound (yield 83%).

^{1}H NMR ($CDCl_3$, 200 MHz): δ (ppm) 7.66 (m, 4H); 7.44 (m, 4H); 7.00 (m, 6H); 6.64 (dd, 2H); 6.43 (dd, 2H), 2.01(broad, 4H); 1.07-0.66 (m, 22H).

^{13}C NMR ($CDCl_3$, 200 MHz): δ (ppm): 152.08; 140.98; 131.94; 130.18; 128.69; 128.04; 126.83; 125.93 123.21; 121.30; 120.94; 120.15; 55.17; 40.54; 31.65; 29.89; 23.94; 22.81; 14.20.

Synthesis of 2,7-(4,4,5,5 – tetramethyl-1,3,2 – dioxaborolan-2-yl)−9,9 – bis(3-(t-butyl propanoate))fluorene (III). The compound was synthesized as described elsewhere.[15,16] Briefly a mixture containing 3.27 g (6.5 mmol) of 2,7-dibromo-9,9-bis(3-(tert-butyl propanoate))fluorene, 2.7 g (27.5 mmol) of KOAc, and 4.2 g (16.5 mmol) of bis(pinacolato)diboron in 40 mL of dry DMF was placed in a flask. After stirring for 20 min under Ar atmosphere, 150 mg of [1,1′-bis(diphenylphosphine)ferrocene] dichloropalladium(II) was added quickly. The mixture was stirred overnight at a temperature of 90°C. After this period, the mixture was cooled, placed in water, and extracted with dichloromethane. The organic phase was then washed with water and dried with $MgSO_4$. After removing the solvent, the residue was purified by column chromatography, yielding compound III as a white solid (yield 68%).

^{1}H NMR ($CDCl_3$, 200 MHz): δ (ppm) 7.80-7.72 (m, 6H); 2.38 (t, 4H); 1.42-1.39 (m, 28H); 1.30 (s, 18H).

^{13}C NMR ($CDCl_3$, 200 MHz): δ (ppm): 172.88; 147.89; 143.83; 134.36; 129.03; 128.40; 119.69; 83.92; 79.97; 53.54; 34.48; 29.99; 28.04; 24.96.

Polymerization. Using a 25 mL flask, 216 mg (0.31 mmol) of 2,7-bis[2-(4-bromophenyl)vinyl]-9,9-dihexyl-9*H*-fluorene (II), 209 mg (0.31 mmol) of 2,7-(4,4,5,5-tetramethyl-1,3,2-dioxaborolan-2-yl)−9,9-bis(3-(t-butyl propanoate))fluorene (III), 8 mg of Pd $(Ph_3P)_4$, and 515 mg (3.7 mmol) of potassium carbonate were mixed. Then, a mixture of water and toluene was added to the flask and Ar was bubbled into the system for 20 min. The mixture was heated to 85°C for 24 hours under Ar and after this period, precipitated in methanol. The polymer was filtered and washed with methanol and acetone. The purification was performed by Sohxlet extraction, yielding a fibrous light yellow solid (yield 57%).

^{1}H NMR ($CDCl_3$, 200 MHz): δ (ppm) 7.70 (broad, 20H); 6.70 (broad, 4H); 2.44 (broad, 8H); 1.80 (broad, 18H); 1.50 (broad, 8H); 1.30 (broad, 12H); 0.75 (broad, 6H).

Equipment

Molar mass distribution was determined by size exclusion chromatography (SEC) using polystyrene standards and THF as solvent at 1 mL/min flow rate in an Agilent 1100 Liquid chromatography system equipped with Plgel Mixed-B and Mixed-C columns and refraction index detector.^{1}H and ^{13}C NMR spectra were recorded in chloroform on a Bruker spectrometer at 200 MHz and room temperature.

The thermal decomposition temperature of the prepared polymer was determined by a Netzsch Thermisch Analyzer TG 209. For the thermogravimetric tests (TGA) a heating rate of 20°C/min was used, with a nitrogen flow of 15 mL/min, from room temperature to 600°C. At 600 C, the purge gas flowing over the sample was automatically switched to synthetic air (80% N_2 and 20% O_2). The DSC equipment used was a Netzsch DSC 204 F1. All the samples were heated from 20°C to 250°C at a rate of 10°C/min in a nitrogen atmosphere, then cooled down to 20°C at 10°C/min. This procedure was repeated and the second run was recorded. Dynamic mechanical analysis was performed in a Netzsch DMA 242C with an amplitude of 10 μm, from −150°C to 200°C at heating rate of 3 K/min at different frequencies, in single cantilever bending mode using a material pocket.[17]

The UV–Vis spectra were taken in a Shimadzu spectrophotometer model NIR 3101. Steady-state fluorescence spectroscopy was performed in a Shimadzu spectrophotometer model RF5301-PC, using a square cuvette of 1 cm path length. The quantum yield was measured using 9,10-diphenylathracene as the standard, following the experimental procedure described by Williams *et al.*[18]

A potentiostat/galvanostat PAR model 273A was used for the electrochemical characterization, with a three-electrode cell. A working electrode (Pt), reference electrode (Ag / Ag^+ in acetonitrile), counter electrode (Pt), a degassed supporting electrolyte (0.1*M* tetrabutyl ammonium hexafluorophosphate in acetonitrile) were used in the measurements with a scanning rate of 50 mV/s. The potentials being referred to the ferrocene/ferrocenium (FcH/FcH^+) pair internal standard.[19,20]

Device Preparation and Characterization. Two types of device structures were adopted in this study: PLEDs and PLECs. Prior to device preparation, the substrates were cleaned with detergent, acetone, and isopropyl alcohol and subsequently underwent a process of hydrophylization with plasma ozone.

A PLED device was built with the ITO/PEDOT : PSS/LaPPS42/Ca : Al structure. First, a layer of PEDOT : PSS (Bayer) was deposited by spin coating at a speed of 3000 rpm, resulting in a 60 nm thick layer. Next, the LaPPS42 was dissolved in chloroform, with 15 mg/mL concentration. Films were obtained from the solutions filtered through 0.2 μm Millex-FGS Filters (Millipore) and deposited by spin coating using a rotation of 3000 rpm, forming films of 70 nm. The calcium cathode and the aluminum was vacuum deposited onto the layer under a pressure of about 10^{-6} mbar resulting in a layer of 20 and 100 nm thick, respectively.

In PLECs, the light-emitting films were prepared by spin-casting the polymers from chloroform/acetonitrile solutions onto an ITO substrate to achieve a film thickness of about 300 nm. Solutions were made using a 10 : 0.1 mass ratio of PEO (polyethylene oxide) to TriLi (lithium triflate), and a 10 : 1 mass ratio of LaPPS42 to total PEO solution. Gold top electrodes were deposited by thermal evaporation following overnight drying under high vacuum (10^{-6} mbar).

The characterization procedures of PLED and PLEC devices were carried out in an InerTec AG glove box, in which the oxygen content was less than 5 ppm (± 1 ppm). The current–voltage measurements were performed using a 2400 Keithley Source. The EL spectra were acquired using an integrating sphere Labsphere model 1100. The luminance–voltage was measured by 238 Keithley connected with a sensible photodiode. The samples were kept in a sealed Janis chamber under high vacuum.

RESULTS AND DISCUSSION

Synthesis and Characterization

Two chemical routes were employed in sequence for the preparation of LaPPS42, as illustrated in Scheme 1. In a first step the fluorene phosphonium salt (I) reacted with the p-bromoaldehyde to form the dibromo derivative (II), following the Wittig route. The latter reacting with the diboronic compound (III) according to a Suzuki cross coupling polycondensation, gave the final polymer LaPPS42.

Compound I was synthesized according to the methodology described by Rodrigues et al. and Turchetti *et al.*[13,14] and after purification it was reacted via Wittig reaction with 1,4-bromobenzaldehyde giving the monomer **II**, which exhibited a yellow color and a strong blue emission. The detailed procedures for the preparation monomer **II** and LaPPS42, through the Suzuki route are described in the literature.[15,21] The number-average and the weight-average molecular weights (Mn and Mw) of the copolymer were determined by SEC, resulting in 31,300 and 96,000 g mol^{-1}, respectively. The polymer presented good solubility in common organic solvents such as tetrahydrofuran, chloroform, dichloromethane, and toluene. These properties facilitate the production of free-standing films.

Electrochemical Properties

To investigate the electrochemical properties, dip-coated films of LaPPS42 were deposited on platinum electrodes and used as working electrode in the traditional three-electrode setup. The cyclic voltammogram of LaPPS42 film is shown in Figure 1. As can be seen, LaPPS42 exhibits only an oxidation process, which starts at 1.3 V (E'_{ox}), as an irreversible process. The oxidation process brings about the rupture of the vinylene linkage, starting a possible "cross-linking" of the polymer or any other degradation mechanism. From the onset oxidation potential (E'_{ox}) determined from the intersection of two tangents drawn as the rising current and baseline charging current of the cyclic voltammetry traces, HOMO energy level was calculated according to the following equation:[22]

$$I_p(E_{HOMO}) = (E'_{ox} + 4.5)eV \quad (1)$$

where I_p is the ionization potential, E'_{ox} is the onset oxidation potential versus the NHE reference electrode. The LUMO level can in principle be calculated using the reduction onset; however, these measurements were difficult to perform reliably for LaPPS42. Therefore, one way to estimate the LUMO energy level is by the use of the optical gap value, according to

$$E_{LUMO} = E_{HOMO} + E_{gap} \quad (2)$$

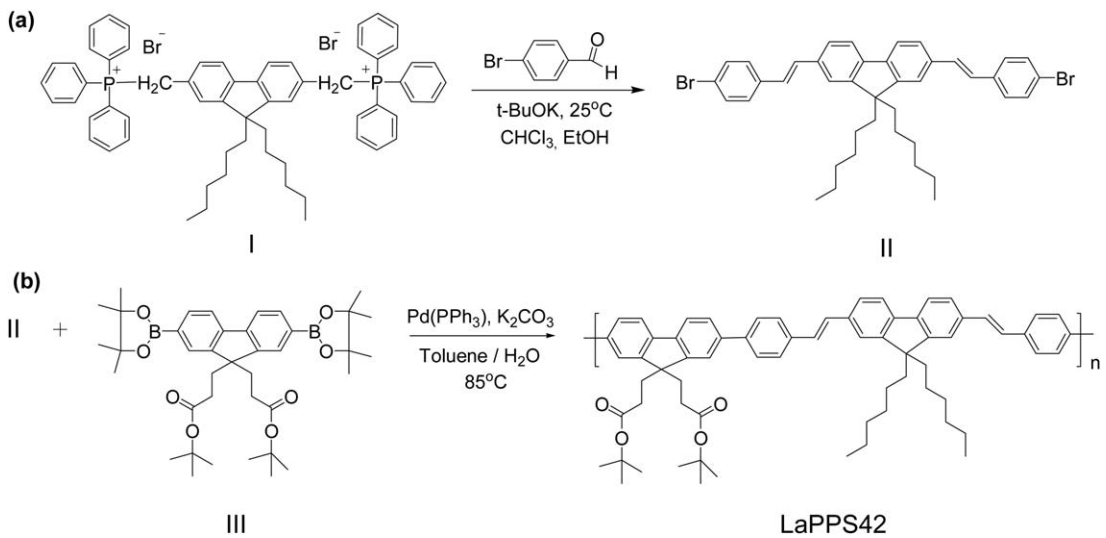

Scheme 1. Schematic representation for the preparation of LaPPS42, following the Wittig (a) and Suzuki (b) routes.

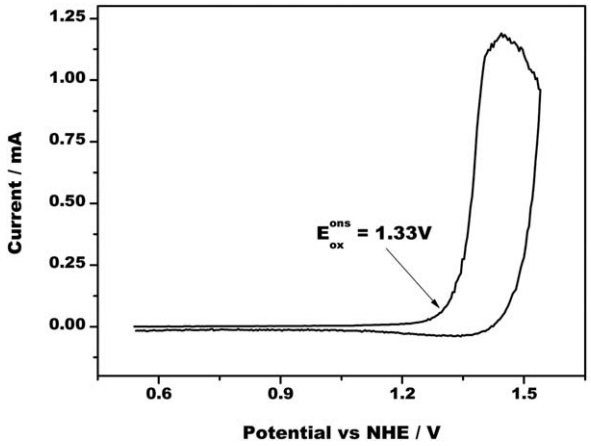

Figure 1. Cyclic voltammogram of LaPPS42 coated on Pt electrode. Supporting Electrolyte: 0.1*M* tetrabutylammonium hexafluorophosphate in acetonitrile. Scan Rate: 50 mVs $^{-1}$.

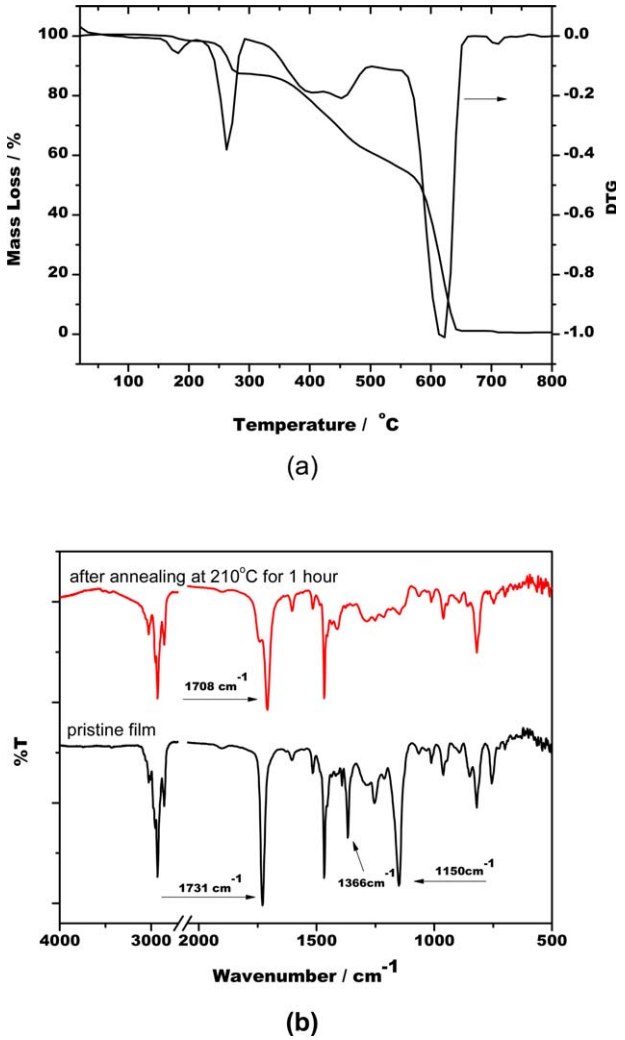

Figure 2. TGA thermogram of (a) LaPPS42 and (b) IR spectra of LaPPS42 film. [Color figure can be viewed in the online issue, which is available at wileyonlinelibrary.com.]

where E_{gap} is the optical band gap, estimated from UV-Vis spectrum (as further shown in Figure 6). Considering that the HOMO energy level and the optical band gap were estimated as −5.8 and 2.7 eV, respectively, the LUMO level was calculated to be −3.1 eV. These energy levels are similar to those reported for polyfluorene derivatives.[19,23]

Thermal Properties

Thermal properties of LaPPS42 were investigated by thermogravimetry analysis (TGA), differential scanning calorimetry (DSC), and dynamic mechanical thermal analysis (DMA). DSC and DMA provide two independent methods to determine phase transitions in polymers by scanning procedures either in the thermal energy uptake or in the mechanical damping of the material.[24]

The thermal stability of the polymer has been investigated by TGA under nitrogen. The TGA traces [Figure 2(a)] presented a first region of mass loss in the range 220–290°C ($\Delta m = 11\%$), which was attributed to the protecting group loss (ester group), leading a formation of carboxylic acid groups (Scheme 2), as corroborated by IR spectroscopy [band at 1366 cm^{-1}, Figure 2(b)]. However, it is possible that the polymer backbone presents a mixture of side groups (carboxylic acid and ester). The absence of a strong broad stretching in the 3000–3500 cm^{-1} region because of the O-H bond could indicate the partial break of the ester bond. The presence of a shoulder at 1731 cm^{-1} (ester) and an intense peak at 1708 cm^{-1} (carboxylic acid) is an indication of this assumption.

Thermocleavable polymers can offer benefits and bring polymer devices to a more advanced level through materials design. A thermocleavable side chain could decrease the density of chromophores in the active layer and improves the morphology of the material, because the alkyl chains are soft and allow for both morphological changes. This behavior is related to the instability of the material, and more rigid systems have proven to give devices with a better stability.[25] The DSC data (Figure 3) show an endothermic process between 210°C and 280°C, attributed to the ester group loss, in agreement with TGA data. The glass transition temperature, obtained in the second run, is about 150°C.

The results provided by dynamical mechanical thermal analysis (DMTA) of LaPPS42 are shown in Figure 4. It can be observed a sudden decrease in storage modulus in the region between 125°C and 170°C because of the occurrence of the cooperative movement of the main chain segments (Tg).[26] In addition, the curve shows an increase of the modulus beyond 230°C, probably associated with the formation of hydrogen bonds between the carboxyl groups, generated after the breaking of the ester group. This breaking causes a slight restriction of the chain movements because of the "physical cross-linking". The loss modulus plot (E'') shows a transition frequency-dependent at 155°C, attributed to the glass transition, coincident with the value observed by DSC measurements.

According to the Arrhenius law, the activation energy for the glass transition was calculated by fitting the frequency f versus $1/T$ of the E'' (Figure 5)[27]:

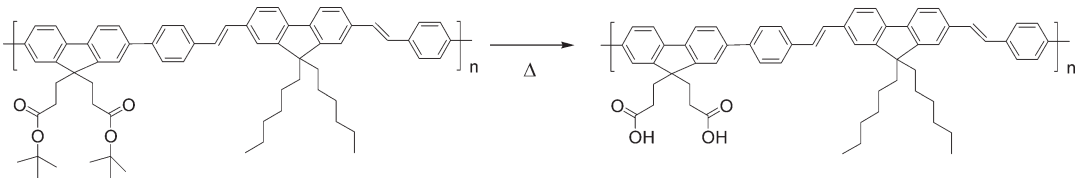

Scheme 2. The thermocleaving reaction.

$$\ln f = \ln f_0 - \frac{E_a}{RT} \quad (3)$$

f is the frequency (Hz), f_0 is the pre-exponential factor (Hz), E_a is the activation energy (J mol^{-1}), T is the absolute temperature where the maximum of tan δ occurs for each relaxation process, and R is 8.32 J K^{-1} mol^{-1}. The calculated activation energy was approximately 595 kJ mol^{-1}.

Optical Properties

The photophysical properties of LaPPS42 were investigated by optical absorption and photoluminescence (PL) spectra of dilute chloroform solution and also by solid film deposited on quartz plate. The results are shown in Figure 6. From the absorption spectra is possible to observe wide absorption for the solution and for the film. One reason for the extension of the absorption process for the film can be assigned as a result of small local variations in π orbital's overlapping because of conformational disorder existing in the material.[28] The analysis of the emission spectra obtained by polymer solution show that they did not vary considerably with the concentration range (from 10^{-7} to 10^{-5} mol L^{-1}). They display a peak and a shoulder, located at 450 and 477 nm, which are related with the stretching mode of C═C─C═C sub-structures of the polymer backbone (electron–phonon coupling),[28] with the 0–0 transition centered at 450 nm. The photoluminescence quantum yield (in solution) was measured to be 65%, using 9,10-diphenylanthracene as the standard. This value is similar to those reported for polyfluorenes derivatives.[29]

The PL spectrum in film shows a red-shift in comparison to those in solutions, with a broader and less resolved structure. This behavior can be attributed to aggregate formation, either in the electronic ground state or in excimeric form.[13,30]

Device Characterization

The electroluminescent spectra of PLECs and PLEDs fabricated with LaPPS42 are shown in Figure 7 and the corresponding PL spectra is presented for comparison. The FWHM of these spectra changes considerably, from 76 nm (PL), 109 nm (EL from PLEC) to 127 nm (EL from PLED). A low-energy band

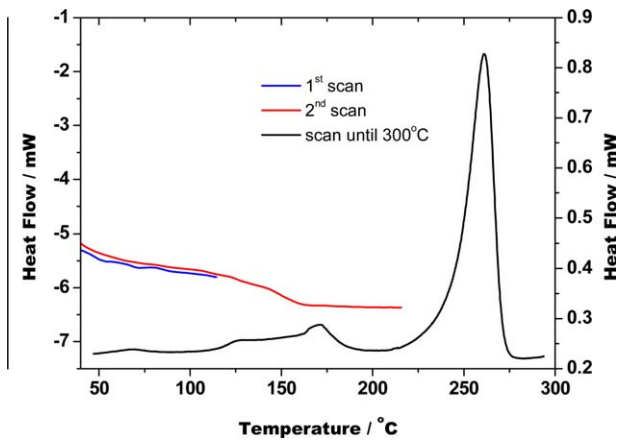

Figure 3. DSC curves of LaPPS42. Scan until 300°C; 1 st and 2 nd scans without ester group loss. [Color figure can be viewed in the online issue, which is available at wileyonlinelibrary.com.]

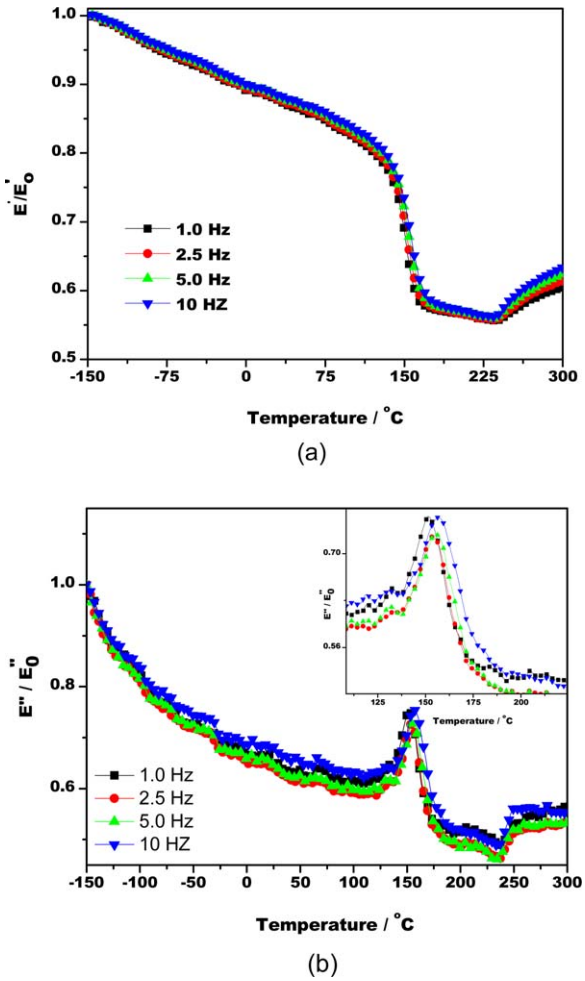

Figure 4. DMA plots of LaPPS42: (a) storage modulus and (b) loss modulus. [Color figure can be viewed in the online issue, which is available at wileyonlinelibrary.com.]

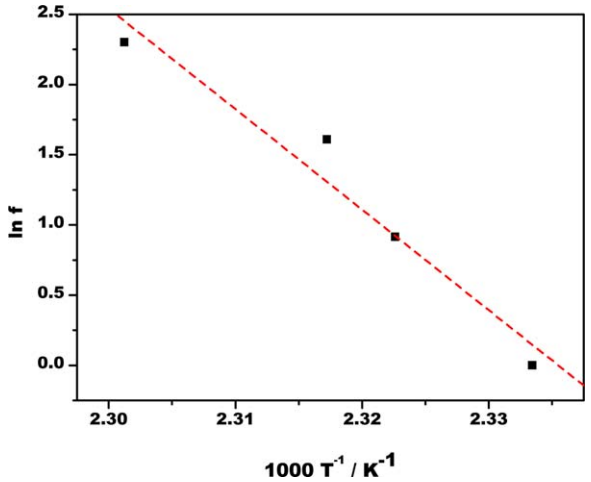

Figure 5. Arrhenius plot for the α relaxation by DMA. [Color figure can be viewed in the online issue, which is available at wileyonlinelibrary.com.]

(centered at 540 nm) is significantly stronger in the EL spectra of the PLED device. This band can be attributed to the presence of the fluorenone defects. It has been proposed[31] that the fluorenone defects are formed because of the reaction of calcium atoms of the cathode with the polyfluorene during the calcium deposition, probably via charge-transfer n-type doping, and the reactive n-doped PF is oxidized to form fluorenone defects.

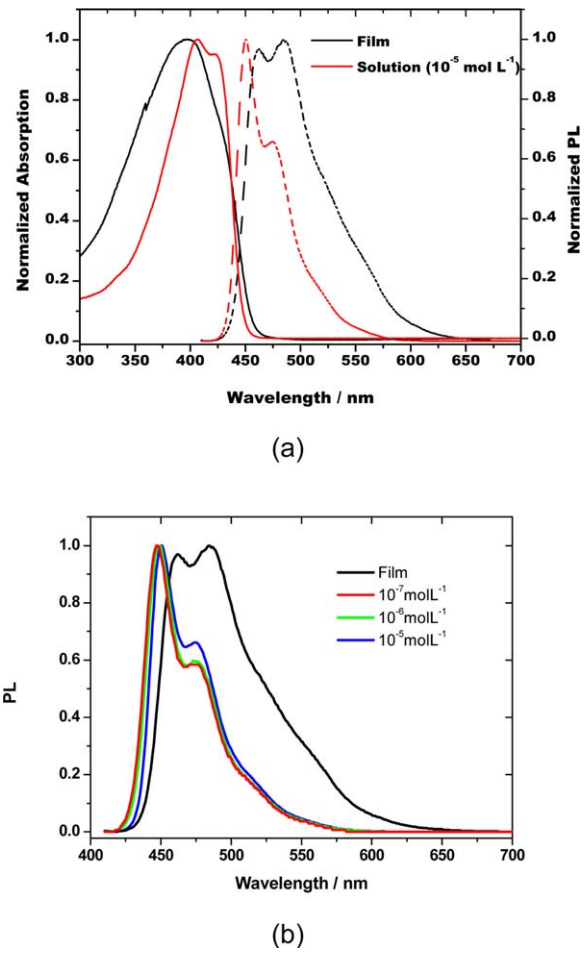

Figure 6. Absorption and emission spectra of (a) LaPPS42 film and solution in $CHCl_3$ and (b) variation of the PL profile with concentration for solutions of LaPPS42 in $CHCl_3$ solution and solid film. [Color figure can be viewed in the online issue, which is available at wileyonlinelibrary.com.]

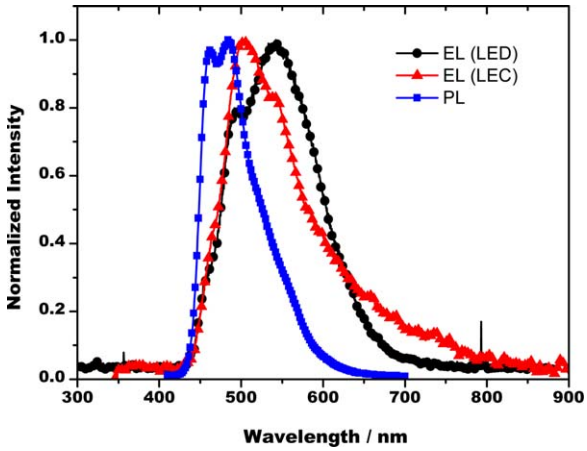

Figure 7. PL and EL spectra of LaPPS42 film and devices. PLED configuration: ITO/PEDOT/LaPPS42/Ca/Al. PLEC configuration: ITO/LaPPS42-PEO-TriLi/Al. [Color figure can be viewed in the online issue, which is available at wileyonlinelibrary.com.]

Other studies reported that calcium can diffuse into the near surface region of polymer to form an interface with bipolaron states within the energy gap of PF. The bipolaron states are detrimental to band–band radiative recombination, because electrons from cathode and holes from anode can recombine at this interface region, especially because the hole mobility of the PF is much higher than the electron mobility.[32,33] As a result, the color of the emission shifts from the desired blue to blue-green.

Particularly, in this work, special attention has to be given to another kind of defects: the possible formation of calcium carboxylate. To try to understand this possibility, new studies using a LiF layer instead of calcium and the characterization of the products generated at the interface polymer / electrode has been done.

According to Figure 8, the PLEC and PLED devices operate with low voltage, showing threshold voltages below to 3.5 V. The PLEC reached 137 Cd/m^2 at 5 V (22 mA/cm^2), whereas the PLED presented 26 Cd/m^2 (1 mA/cm^2) at same voltage. The PLED showed a slightly higher performance compared to the PLEC. Under a voltage of 4 V the PLED luminance efficiency (Cd/A) was five times higher than that exhibited by the PLEC. Although the results are initials, the device performance is reasonably in comparison with other polyfluorene homopolymers and derivatives,[34,35] indicating that this new PPV-fluorene structure is a promising candidate for the development of efficient electroluminescent polymers, in a PLED or a PLEC configuration.

The differences observed in the behavior of EL of the PLEC devices, in comparison to PL spectrum (Figure 7), can be attributed to the presence of radiative traps of chemical or physical origin that affect the EL more than the PL. The reason is that charge carriers, injected from the electrodes, have to migrate into the bulk of the dielectric in order to react and therefore

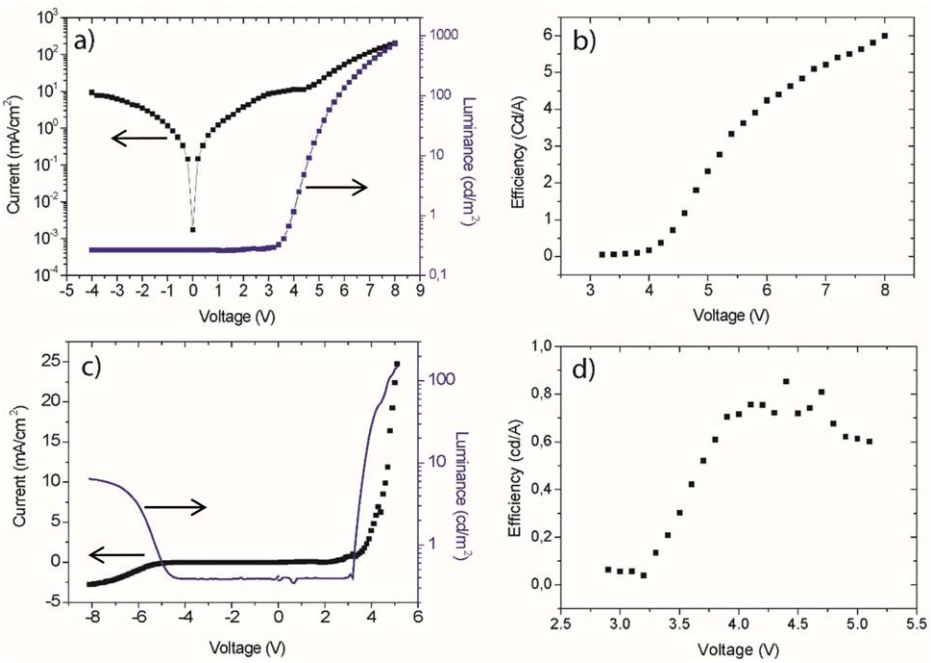

Figure 8. *I vs V* and *L vs V* plots for the PLED (a, b) and PLEC (c, d) devices. [Color figure can be viewed in the online issue, which is available at wileyonlinelibrary.com.]

have a much higher chance of becoming trapped at a radiative or nonradiative defect than short-lived singlet excitons.[36]

CONCLUSIONS

The electrochemical, thermal, dynamical thermomechanical, and photoluminescence properties of LaPPS42 pointed out to a material with a band gap of 2.7 eV, that undergoes thermal cleavage of its ester groups yielding carboxyl groups which increase moduli and thermal resistance, probably because of hydrogen bond formation or cross-linking. The photo-physical characterization indicated a tendency to aggregation in going from dilute to concentrated conditions, with strong redshift and broadening for film form. The EL spectra of PLEC and PLEDs fabricated with LaPPS42 showed differences when compared to the corresponding PL, because of dissimilar mechanisms in the operation of the devices, notably the presence of traps resulting in different *loci* of recombination. The performance of these first devices are promising when compared with other carried out with polyfluorene homopolymer and derivatives, indicating that this new PPV-fluorene structure can be more explored to fabricate efficient electroluminescent polymers, using a PLED or a PLEC configuration.

ACKNOWLEDGMENTS

The authors gratefully acknowledge the funding from FAPESP (2011/08463-4), CNPq and the National Institute for Science and Technology on Organic Electronics (INEO).

REFERENCES

1. Akcelrud, L. *Prog. Polym. Sci.* **2003**, *6*, 875.
2. Xiao, H.; Yu, l.; Li, Y.; Yang, W.; Zhang, B.; Yang, W.; Wu, H.; Cao, Y. *Polymer* **2012**, *53*, 2873.
3. Tan, Y.; Gu, Z.; Tsuchiya, K.; Ogino, K. *Polymer* **2012**, *53*, 1444.
4. Peng, Z.; Tao, S.; Zhang, X.; Tang, J.; Lee, C. S.; Lee, S. T. *J. Phys. Chem. C* **2008**, *112*, 2165.
5. Helgesen, M.; Bjerring, M.; Nielsen, N. C.; Krebs, F. C. *Chem. Mater.* **2010**, *22*, 5617.
6. Friend, R. H.; Gymer, R. W.; Holmes, A. B.; Burroughes, J. H.; Marks, R. N.; Taliani, C.; Bradley, D. D. C.; Dos Santos, D. A.; Bredas, J. L.; Logdlund, M.; Salaneck, W. R. *Nature* **1999**, *397*, 121.
7. Kraft, A.; Grimsdale, A. C.; Holmes, A. B. *Angew. Chem. Int. Ed.* **1998**, *37*, 402.
8. de Deus, J. F.; Faria, G. C.; Iamazaki, E. T.; Faria, R. M.; Atvars, T. D. Z.; Akcelrud, L. *Org. Electron.* **2011**, *12*, 1493.
9. Shao, Y.; Bazan, G. C.; Heeger, A. *J. Adv. Mater.* **2008**, *20*, 1191.
10. Pei, Q.; Yang, Y.; Yu, G.; Zhang, C.; Heeger, A. J. *J. Am. Chem. Soc.* **1996**, *118*, 3922.
11. Gozzi, G.; Faria, R. M.; Santos, L. F. *Appl. Phys. Lett.* **2012**, *101*, 113305.
12. Gozzi, G.; Faria, R. M.; Santos, L. F. *EPL* **2012**, *100*, 18001.
13. Rodrigues, P. C.; Grova, I.; Coutinho, D. J.; Domingues, R. A.; Oh, H. S.; Seo, J.; Faria, R. M.; Atvars, T. D. Z.; Prasad, P. N.; Akcelrud, L. *J. Polym. Res.* **2012**, *19*, 9828.
14. Turchetti, D. A.; Rodrigues, P. C.; Berlim, L. S.; Zanlorenzi, C.; Faria, G. C.; Atvars, T. D. Z.; Schreiner, W. H.; Akcelrud, L. *Synth. Met.* **2012**, *162*, 35.
15. Liu, X.; Zhu, R.; Zhang, Y.; Liu, B.; Ramakrishna, S. *Chem. Commun.* **2008**, *32*, 3789.

16. Rodrigues, P. C.; Berlim, L. S.; Azevedo, D.; Saavedra, N. C.; Prasad, P. N.; Schreiner, W. H.; Atvars, T. D. Z.; Akcelrud, L. *J. Phys. Chem. A* **2012**, *116*, 3681.
17. Hopkinson, P. E.; Staniec, P. A.; Pearson, A. J.; Dunbar, A. D. F.; Wang, T.; Ryan, A. J.; Jones, R. A. L.; Lidzey, D. G.; Donald, A. M. *Macromolecules* **2011**, *44*, 2908.
18. Williams, A. T. R.; Winfield, S. A.; Miller, J. N. *Analyst* **1983**,*108*, 1067.
19. Admassie, S.; Inganas, O.; Mammo, W.; Perzon, E.; Andersson, M. R. *Synth. Met.* **2006**, *156*, 614.
20. Gritzner, G.; Kuta, J. *Pure Appl. Chem.* **1984**, *56*, 461.
21. Correa, D. S.; De Boni, L.; Nowacki, B.; Grova, I.; Fontes, B. D.; Rodrigues, P. C.; Tozoni, J. R.; Akcelrud, L.; Mendonça, C. R. *J. Polym. Sci. B Polym. Phys.* **2012**, *50*, 148.
22. Pavlishchuk, V. V.; Addison, A. W. *Inorg. Chim. Acta* **2000**, *298*, 97.
23. Perzon, E.; Wang, X.; Admassie, S.; Inganäs, O.; Andersson, M. R. *Polymer* **2006**, *47*, 4261.
24. Friedel, B.; McNeill, C. R.; Greenham, N. C. *Chem. Mater.* **2010**, *22*, 3389.
25. Helgesen, M.; Søndergaard, R.; Krebs, F. C. *J. Mater. Chem.* **2010**, *20*, 36.
26. Faria, G. C.; Cossiello, R. F.; Atvars, T. D. Z.; deAzevedo, E. R. *Synth. Met.* **2009**, *159*, 2289.
27. Bernardinelli, O. D.; Faria, G. C.; Nunes, L. A. O.; Faria, R. M.; deAzevedo, E. R.; Pinto, M. F. S. *J. Phys. Chem. A* **2012**, *116*, 4285.
28. Scherf, U.; List, E. J. W. *Adv. Mater.* **2002**, *14*, 477.
29. Marques, A. T.; Burrows, H. D.; de Melo, S. S.; Valente, A. J. M.; Justino, L. L. G.; Scherf, U.; Fron, E.; Rocha, S.; Hofkens, J.; Snedden, E. W.; Monkman, A. P. *J. Phys. Chem. B* **2012**, *116*, 7548.
30. Oliveira, H. P. M.; Martins, T. D.; Honório, K. M.; Rodrigues, P. C.; Akcelrud, L.; Silva, A. B. F.; Atvars, T. D. Z. *J. Braz. Chem. Soc.* **2009**, *20*, 160.
31. Gong, X.; Iyer, P. K.; Moses, D.; Bazan, G. C.; Heeger, A. J.; Xiao, S. S. *Adv. Funct. Mater.* **2003**, *13*, 325.
32. Liao, L. S.; Cheng, L. F.; Fung, M. K.; Lee, C. S.; Lee, S. T.; Inbasekaran, M.; Woo, E. P.; Wu, W. W. *Chem. Phys. Lett.* **2000**, *325*, 405.
33. Salaneck, W. R.; LoÈgdlund, M. *Polym. Adv. Technol.* **1998**, *9*, 419.
34. Fallahi, A.; Taromi, F. A.; Mohebbi, A.; Yuenc, J. D.; Shahinpoor, M. *J. Mater. Chem. C* **2014**, *2*, 6491.
35. Tang, C.; Xu, H.; Liu, F.; Liu, X.-D.; Lai, W.-Y.; Wang, X.-L.; Huang, W. *Synth. Met.* **2013**, *174*, 33.
36. Uckert, F.; Tak, Y.-H.; Müllen, K.; Bässler, H. *Adv. Mater.* **2000**, *12*, 905.